Springer

KSME

Journal of Mechanical Science and Technology 00 (2012) 0000~0000
www.springerlink.com/content/1738-494x

Novelty detection methods for online health monitoring and post data analysis of turbopumps

Hu Lei[1,*], Hu Niaoqing[1], Zhang Xinpeng[1], Gu Fengshou[2] and Gao Ming[3]

[1] *Laboratory of Science and Technology on Integrated Logistics Support, College of Mechatronics and Automation, National University of Defense Technology, Changsha, 410073, China*
[2] *School of Computing and Engineering, University of Huddersfield, Huddersfield, HD1 3HD, United Kingdom*
[3] *Research Management Office, College of Mechatronics and Automation, National University of Defense Technology, Changsha, 410073, China*

(Manuscript Received 000 0, 2012; Revised 000 0, 20121; Accepted 000 0, 2012)

Abstract

As novelty detection works when only normal data are available, it is of considerable promise for health monitoring in cases lacking fault samples and prior knowledge. In this paper, two novelty detection methods are presented for health monitoring of turbopumps in large-scale liquid-propellant rocket engines. The first method is the adaptive Gaussian threshold model. This method is designed to monitor the vibration of the turbopumps online because it has minimal computational complexity and is easy for implementation in real time. The second method is the One-Class Support Vector Machine (OCSVM) which is developed for post analysis of historical vibration signals. Via post analysis the method not only confirms the online monitoring results but also provides diagnostic results so that faults from sensors are separated from those actually from the turbopumps. Both of these two methods are validated to be efficient for health monitoring of the turbopumps.

Keywords: Novelty detection; Health monitoring; Turbopump; Gaussian threshold model; One-class support vector machine

1. Introduction

Health monitoring is of importance for turbopumps of large-scale liquid-propellant rocket engines. As the turbopump is one of the primary machineries for the engine, any unanticipated events would lead to damages to the system or even to failure of the whole engine system. Vibration is a cause of turbopump destructions and hence it provides useful information about the health of the turbopumps. Thus vibration based methods can be utilized to monitor the turbopumps to give warning of any abnormal operation.

Large amounts of vibration datasets have been recorded from different ground tests performed over several years. As faults occurred, the engines either were shut down in a timely manner or the engines failed. Though they were occasions when some faults were found in the systems, it has been reported that most of these datasets are from normal operating states. In this scenario because of the lack of fault samples and prior knowledge, a health monitoring system cannot be trained on all possible state patterns. Thus the recognition of novel or unknown states turns out to be a challenge. Novelty detection is the identification of new or unknown data that a machine learning system is not aware of during training [1-2]. As novelty detection methods are able to work where only normal data are available, such methods are of considerable promise for health monitoring in cases lacking fault samples and prior knowledge.

Novelty detection methods that have been used in health monitoring include probability/density estimation methods [2-5], immune system based methods [6], neural networks [2, 7-8], support vector methods [5, 9-10], etc. Markou and Singh made outstanding reviews on these methods [1, 11]. As for the turbopumps of liquid-propellant rocket engines, a support vector based novelty detection method showed superior performance in giving warning of several kinds of novelties [12]. In addition, it has been found that there are problems with the mounting of piezoelectric accelerometers in several occasions due to excessive levels of vibration or huge shocks. Applying OCSVMs to turbopump health monitoring showed that sensor faults were identified as novel events too. Thus sensor faults

*Corresponding author. Tel.: +82 0731 84574971
E-mail address: lake_hl@hotmail.com
† Recommended by Editor

should be recognized; otherwise they can be misinterpreted as turbopump faults and lead to false alarms.

In this paper, two novelty detection methods are investigated for health monitoring of the turbopumps. One is the adaptive Gaussian threshold model which is used for the online health monitoring of the turbopumps. The other is the OCSVM which is implemented for the off-line post analysis to diagnose different types of faults.

2. Online health monitoring

Online health monitoring aims at finding the faults from the turbopumps in time and taking actions accordingly to prevent the turbopumps from any severe damages during ground tests. Each turbopump is tested only once and each test is performed on a specified turbopump. The ground test of each turbopump lasts as long as 500 seconds. When a sampling frequency of f_s is 50 000 Hz, a large dataset needs to be processed for fault detection. In order to ensure timely response to any abnormal events, the online monitoring algorithm must have minimal computational complexity for fast implementation. As statistical results show that the underlying distribution of vibration features is Gaussian when the turbopumps are normal, statistical features and an adaptive Gaussian threshold model are selected for the online health monitoring of the turbopumps.

The Gaussian threshold model is one of the simplest algorithms used widely for novelty detection. However, if the input vector is multi-dimensional, founding a Gaussian threshold model requires calculation of the inverse of the covariance matrix, and sometimes the pseudo-inverse of the covariance matrix [13]. In order to avoid computational effort of the inverse matrix, features will be modeled separately and a novel index will be defined.

2.1 Feature selection for online health monitoring

The turbopumps of liquid-propellant rocket engines are rotating machines. The rotor of each turbopump consists of a shaft and some rotating components fixed on the shaft. Such rotating components include a turbo wheel, three centrifugal wheels of pumps, and bearings, as shown in Fig.1. Both the turbo and the pumps have a number of uniformly spaced blades or vanes on the rotor. Typical faults of the turbopump rotor system include rub-impact between rotor and stator, blade cracks, blade shedding, rotor unbalance, rotor misalignment, rotor bow, etc. One of these kinds of faults could be the cause or effect of another kind of faults. Examples are as follows. A misaligned rotor will be bent with bearing housing leading to rotor bow, while a bent rotor leads to unbalance. Blade shedding will cause unbalance too. Rub-impact often goes along with unbalance and thermal misalignment.

Because of the limitation of space in the turbopump's structure, three accelerometers are mounted externally as shown in Fig 1. Measured vibration signals will contain not only excitations form the rotor but also excitations from other components of the rocket engine. The signals have broadband

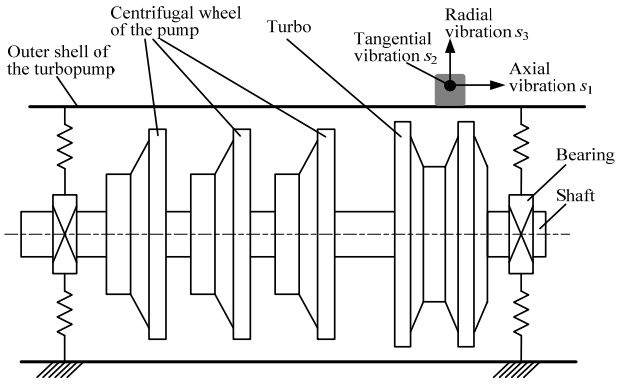

Fig. 1. Schematic illustration of turbopump and vibration measurements in tri-axial directions.

frequency components and feature frequencies used for fault identification can be masked by noise. Therefore, it is difficult to recognize turbopump faults based on the frequency domain features.

It should be noted that these turbopumps are not reusable and their service lives are very short, so weak faults that evolve slowly will not cause breakdown during the turbopumps' service lives. Thus weak faults and powerful signal processing techniques used to extract weak fault features are not addressed. The online monitoring aims at only sudden changes which can be caused by blade damage, rub-impact, and sudden unbalance. Introductions of these damage scenarios are as follows.

(1) Blade damage. Rotating blades interact with components on the stator to give a periodic excitation to the casing. When the rotor runs in a healthy state, the interactions between blades and stator components are relatively small. However, if one or two blades are damaged, the flow angles of liquid-propellant will change and more impulsive interactions will be created. Increased impulsive interactions give increased excitations to the casing. Then vibration will change in the form of energy and statistical features.

(2) Rub-impact. Rub-impact between rotor and stator is very destructive, especially for high-power machinery such as the turbopump. The vibration phenomena of rub-impact have been studied [14-15]. Excessive unbalance, thermal misalignment, changing stiffness and nonlinear phenomena can be caused during rub-impact. The vibration level becomes high. At the same time, periodic impacts and frictions lead to spikes or peaks in vibration signals.

(3) Unbalance. Mass unbalance is a common cause of rotor vibration as mass unbalance can never be reduced to zero. When the rotor runs at a steady rotational speed which is far higher than the second order critical rotational speed, the additional vibration caused by unbalance is quite small. However, a sudden unbalance which may be caused by blade shedding or loosening of rotor components, gives the casing a sudden additional excitation.

All the above kinds of faults which we are concerned about change the level and the waveform of vibration. The change

of vibration level can be described with root mean square (RMS) x_r. RMS increases with the presence of increasing vibration level.

The waveform of vibration signals can be described with statistical features such as kurtosis factor and crest factor. The kurtosis factor x_k is defined as the fourth moment normalized by the square of the variance [16]. The kurtosis measures the difference of peakedness/flatness between a random distribution and the Gaussian distribution. The crest factor x_c is defined as the ratio of the maximum absolute value and the RMS x_r. The crest factor is a normalized measure of the vibration amplitude and it increases in the presence of a small number of high-amplitude spikes or peaks [16]. These two features are able to detect spikes that may be caused by impacts, shocks or friction when faults of rub-impact, blade shedding or unbalance happen.

The number of vibration samples used to calculate each feature sample is set to be N = 5 000, which means that the time interval between two successive feature samples is $\Delta t = N/f_s$ = 0.1 second. The authors and field engineers have found that this time frame is acceptable for the requirement of time accuracy.

2.2 Adaptive Gaussian threshold model

Statistical results show that the distribution of selected features (RMS, kurtosis factor, or crest factor) is Gaussian. For a feature x, if its mean and standard deviation are supposed to be μ and σ, according to Chebyshev's inequality, for any $\varepsilon > 0$, the following inequality holds:

$$P(|x-\mu|\geq\varepsilon)\leq\frac{\sigma^2}{\varepsilon^2},\ \forall\varepsilon>0 \tag{1}$$

By denoting $\varepsilon = k\sigma$, inequality (1) can be rewritten as

$$P(|x-\mu|\geq k\sigma)\leq k^{-2},\ \forall k>0 \tag{2}$$

The above inequality means that the probability of $x\in(\mu-k\sigma, \mu+k\sigma)$ is bigger than $1-k^{-2}$. k is called threshold tolerance. The above inequality is called three sigma criterion when k = 3.

If x_t is the sample extracted at time t, for online monitoring algorithms, x_t is tested using the detection model trained on training set $\{x_{t-L}, \ldots, x_{t-1}\}$, where L is the training set size. The mean and the standard deviation of this training set can be estimated by

$$\bar{x}_{t-1}=\frac{1}{L}\sum_{j=t-L}^{t-1}x_j \tag{3}$$

$$D_{t-1}=\sqrt{\frac{1}{L-1}\sum_{j=t-L}^{t-1}\left(x_j-\bar{x}_{t-1}\right)^2} \tag{4}$$

where $\bar{x}_{t-1}$ and D_{t-1} are estimated mean and estimated standard deviation at time $t-1$. Then for a given threshold tolerance k, the threshold interval can be constructed as

$$C_{t-1}=\left[\bar{x}_{t-1}-kD_{t-1},\ \bar{x}_{t-1}+kD_{t-1}\right] \tag{5}$$

Thus a decision function at time t can be obtained as

$$f_t(x_t)=-\left|x_t-\bar{x}_{t-1}\right|+kD_{t-1} \tag{6}$$

which allows the novelty detection to be implemented explicitly. In particular, $f_t(x_t) \geq 0$ means x_t is normal whereas $f_t(x_t) < 0$ means x_t is novel.

Moreover, for the case of $f_t(x_t) \geq 0$, the training set is updated from $\{x_{t-L}, \ldots, x_{t-1}\}$ to $\{x_{t-L+1}, \ldots, x_t\}$ and the decision function $f_{t+1}(x_{t+1})$ is reconstructed accordingly. For better computational efficiency, $\bar{x}_t$ and D_t is calculated using a recursive method by Eqs. (7) and (8) rather than using Eqs. (3) and (4).

$$\bar{x}_t=\frac{1}{L}\sum_{j=t-L+1}^{t}x_j=\bar{x}_{t-1}+\frac{1}{L}\left(x_t-x_{t-L}\right) \tag{7}$$

$$D_t\approx D_{t-1} \tag{8}$$

Replacing ($\bar{x}_{t-1}$, D_{t-1}) in Eq. (6) with ($\bar{x}_t$, D_t) yields decision function at time t+1:

$$f_{t+1}(x_{t+1})=-\left|x_{t+1}-\bar{x}_t\right|+kD_t \tag{9a}$$

If $f_t(x_t) < 0$, x_t is considered to be novel or abnormal. In this case, x_t is not added to the training set to replace x_{t-L}, neither the decision function is reconstructed as above. But the decision function at time t is applied to x_{t+1} as

$$f_{t+1}(x_{t+1})=-\left|x_{t+1}-\bar{x}_{t-1}\right|+kD_{t-1} \tag{9b}$$

This means that novel samples do not make any contribution to the updating of the detection algorithm and the threshold model adapts only to the normal data.

Applying adaptive Gaussian threshold model to each of features yields outputs of the model $f_{i,t}(x_{i,t})$. The subscript i =1, 2 and 3 denotes RMS, kurtosis factor and crest factor respectively, and the subscript t denotes that the samples and the outputs of the model are at time t.

To obtain a unified threshold, novelty indexes of each signal are defined and can be written as

$$I_t=\sum_{i=1}^{3}f_{i,t}(x_{i,t}) \tag{10}$$

$I_t \geq 0$ denotes that the vibration is normal and $I_t < 0$ means that the vibration is novel.

This model requires the selection of two parameters, in particular the threshold tolerance k and the training set size L. The threshold tolerance k is determinative to balance false negative and false positive. According to Eq. (2) and Eq. (5), the larger the k is, the wider the threshold interval is and hence the smaller probability that the normal samples exceed the threshold intervals, which means that the system has fewer false negatives. Conversely, the smaller the k is, the narrower the threshold interval is and the smaller probability that the novel samples are located in the threshold intervals, which means that the system is more sensitive. So k can be set with cross validation as follows: (1) Initialize k to be 3 or any value; (2) If monitoring results of historical data show unacceptable false negative alarms, increase k; (3) On the contrary, if monitoring results of historical data show unacceptable false positive rate, reduce k; (4) False negative rate and false positive rate cannot be reduced simultaneously, a balance between them should be reached. For field engineers of the rocket engine, a high false negative rate is more intolerable than high false positive rate.

Fig.2 displays the false negative rates and the false positive rates at different threshold tolerance. Fig.2 shows that a relative bigger k = 5 is an optimized selection for online health monitoring of the turbopumps.

The training set size L can be adapted so that it is in accordance with the dynamics of the monitored process. For example, in music processing, L can be adapted so that each training set spans 54.4 milliseconds, which is a standard frame length in music processing. In health monitoring of gearbox wheel, if the vibration signal is resampled with equal angle intervals, L can be adapted so that each feature sample carries the information concerning a single tooth, and every tooth is represented only once in the training set [17]. For the turbopumps, the training set size L cannot be selected in the same way as for gearbox wheels unless the vibration signal is resampled with equal angle intervals. In this paper, we don't perform resample. First of all, resample introduces additional computational load. Secondly, selection of the training set size L is not decisive of the monitoring results. Monitoring results presented in section 2.3 show that the monitoring model works well when the training set size is selected as L = 30.

2.3 Monitoring results

Three piezoelectric accelerometers are used to measure vibrations of the turbopump during ground tests. These sensors are mounted to the casing of the turbopump, as shown in Fig. 1. These three sensors are used respectively to measure axial vibration signal s_1, tangential vibration signal s_2 and radial vibration signal s_3. Vibration signals at three directions are sampled at 50 000 Hz synchronously.

When the ground test starts, the rotational speed of the turbopump will increase from zero to a specified steady rotational speed in 3 seconds. During the transient speedup process, the turbopump passes the first order critical rotational speed and the second order critical rotational speed. The first/second order critical speed is the angular velocity that excites the first/second order natural frequency of the turbopumps. As critical speeds approach natural frequencies, the turbopumps begin to resonate and the instantaneous vibration increases significantly. Great deviations of the time domain features will be caused and lead to false alarms. Thus the online health monitoring method used in this paper is not applied during the speedup transient process. The training set size is set to be L = 30. So the training set spans $\Delta t \cdot L$ = 3 seconds and it will take 3 seconds to initialize the adaptive threshold model. Thus the monitoring is effective until 6 seconds later after the test started.

Figure 3 shows the detection results of the axial vibrations of the turbopump during a test numbered as T627. Test T627 lasts only 12.8 seconds since vibration level increased sharply at 11.7 seconds. The appearance of rub-impact fault was identified by field engineers via disassembly and check. Fig. 3a to 3d present the detection details of these features and the novelty indexes respectively. The solid lines in Fig. 3a to 3c are the time domain features and the dotted lines are the thresholds of these features whereas the solid line in Fig. 3d denotes the novelty indexes and the dotted line denotes the thresholds of the indexes. It can be seen clearly that features go out of the thresholds after 11.7 seconds. The kurtosis factors and the crest factors show higher amplitudes at the beginning of the faults and they become lower as time goes by. In contrast, the RMS values become larger and larger after 11.7 seconds. Novelty indexes jump sharply at 11.7 seconds and become negative. Negative novelty indexes indicate novelties, which is consistent with the fault state of the turbopump. This instance demonstrates that the designed method produces the expected detection performance.

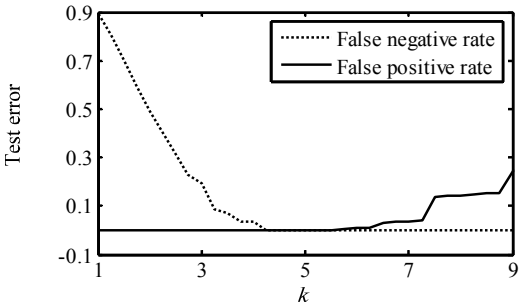

Fig.2. Change of test error at different threshold tolerance

Figure 4 shows the detection results of the tangential vibrations in another test instance numbered as T618. The tested turbopump itself was confirmed to be normal. However, several novelties are detected at about 91.9 seconds and 104.1 seconds. These novelties are found due to moment malfunction of the accelerometer at tangential direction. This instance shows that the algorithm also gives alarms to novelties caused by sensor faults. This instance will be discussed further in section 3.

2.4 Discussion

Traditionally a novelty detector is first trained with a fixed training set and then it is applied to new datasets for detecting any possible novelties. However, the adaptive Gaussian threshold model developed in this paper is trained online adaptively for more accurate and yet robust novelty detection. As derived in section 2.2, the training dataset is updated at each step by removing the earliest data point and including the latest data point. This online learning strategy enables the model to be adaptive to gradual changes or drifts in features and avoid false alerts due to such changes. In most cases, these gradual changes may be from environmental effects such as temperature increasing. On the other hand, the gradual change does happen in many machines because of the slow deterioration with their service life. However, as mentioned in section 2.1, the turbopump is not reusable and its service life is very short. The deterioration process in mechanical parts is not likely to end in failure before the service life is over. Therefore, the model developed in this study is particularly applicable to

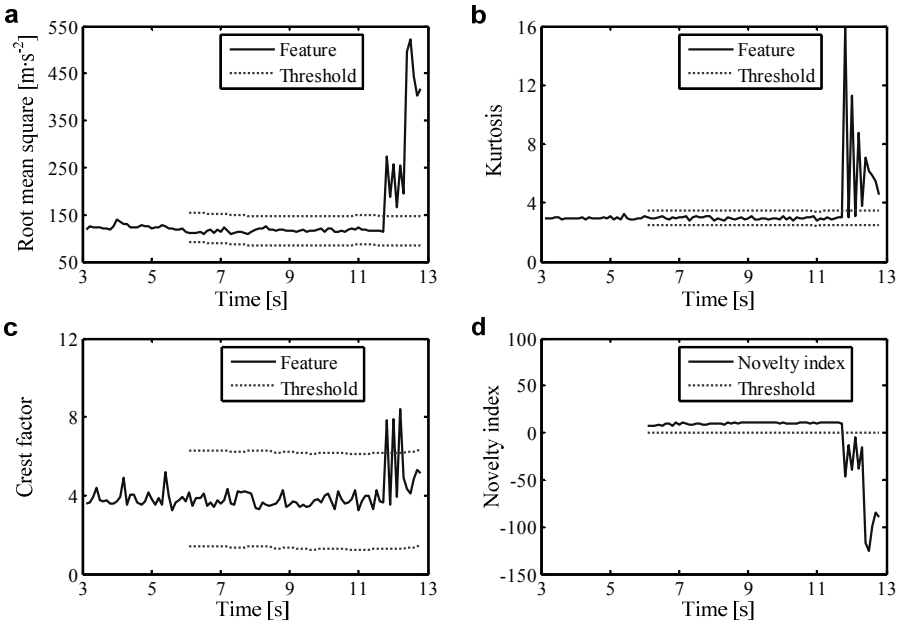

Fig.3. Detection results of the axial vibration in test T627.

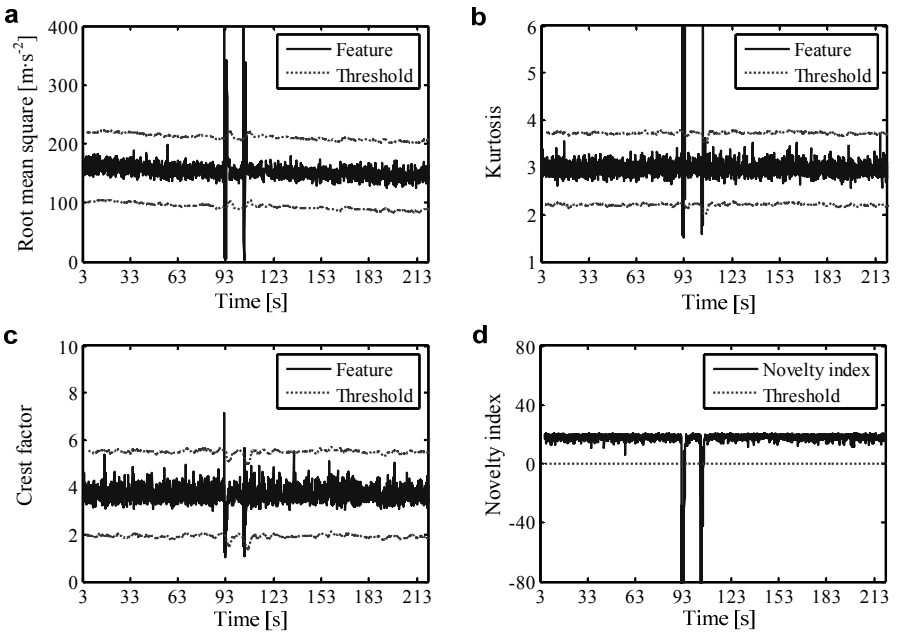

Fig.4. Detection results of the tangential vibration in test T618.

special machines such as the turbopump with short service life or more suitable to detect rapid changes in a common machine operation but not for monitoring machines with a long term deterioration processes.

In addition, the adaptive Gaussian threshold model developed in this study is different from that in Ref. [18]. Although the algorithm in Ref. [18] was also named adaptive threshold algorithm, an incremental learning strategy was actually adopted and its implementation needs more computational work. In particular, when a new data point x_t is included into the training set, the earliest one x_{t-L} is not removed. This means that the training set is updated into $\{x_{t-L}, \ldots, x_t\}$ rather than $\{x_{t-L+1}, \ldots, x_t\}$ and the estimated mean and estimated standard deviation at time t are updated as follows [18].

$$\bar{x}_t = \frac{1}{L+1}\sum_{j=t-L}^{t} x_j = \frac{L}{L+1}\bar{x}_{t-1} + \frac{1}{L+1}x_t \tag{11}$$

$$D_t = \sqrt{\frac{1}{L}\sum_{j=t-L}^{t}(x_j - \bar{x}_t)^2}$$
$$\approx \sqrt{\frac{L-1}{L}(D_{t-1})^2 + \frac{1}{L+1}(x_t - \bar{x}_{t-1})^2} \quad (12)$$

Computing Eqs. (7) and (8) is easier than computing Eqs. (11) and (12). Moreover, the adaptive threshold model developed in this study produces threshold intervals more adaptive than the incremental learning model developed in Ref. [18]. Fig.5 shows the detection results of statistical features with the adaptive model and the incremental learning model. Solid lines are crest factors and dotted lines are the thresholds of these features. Fig. 5(b) shows that the incremental learning model produces increasing threshold intervals. As a wider threshold means a less sensitive detection model, the incremental learning model becomes less and less sensitive during a test. While Fig. 5(a) shows that the breadth of the threshold intervals produced with adaptive threshold model are fixed. The adaptive threshold model has persistent sensitivity to sudden changes caused by faults.

3. Post analysis

The post analysis of history test data aims at a further validation of the turbopump health. As computational efficiency demand for the post analysis is not as critical as for the online monitoring, more advanced pattern recognition methods and signal processing techniques can be utilized to diagnose the natures of faults. In this study, OCSVM is selected for separating the faults of the turbopumps from sensor faults.

3.1 Feature selection for sensor fault description

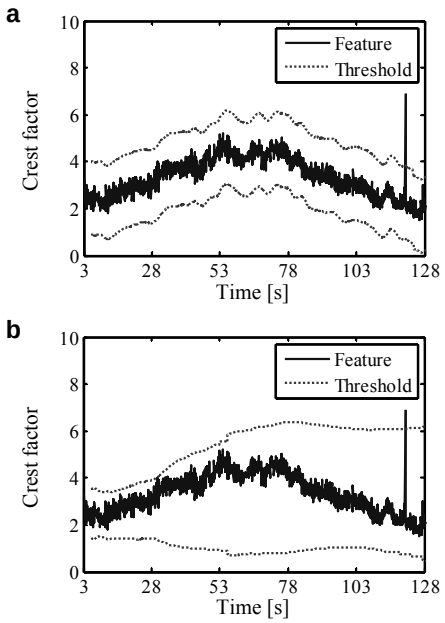

Fig.5. Comparison between (a) adaptive learning and (b) incremental learning.

Sensors may have abnormalities like bias, drifting, precision degradation, gain variation, etc. Such faults can be detected and corrected in a multichannel measurement system with enough redundant sensors [19]. However, the sensor fault of the turbopump is a different type of malfunction. Fig. 6 shows partial typical waveform of the tangential vibration in test T618. There is an excessive negative shock at about 91.9 seconds. Then the accelerometer seems to have little output until 93.3 seconds. This abnormal phenomenon also appeared at 104.1 seconds during test T618.

Components of vibration from the turbopump cannot be well sampled during sensor malfunction, and the vibration signal becomes weak random noise. Fig. 7a and 7b show the amplitude spectra of the vibration before and after the sensor malfunction respectively. It can be seen from Fig. 7b that there is only a 0 Hz DC component and its leakage when the sensor is in malfunction. On the contrary, there are abundant components in the frequency band from 3 000 Hz and 7 000 Hz for the normal sensor case. To describe this difference between

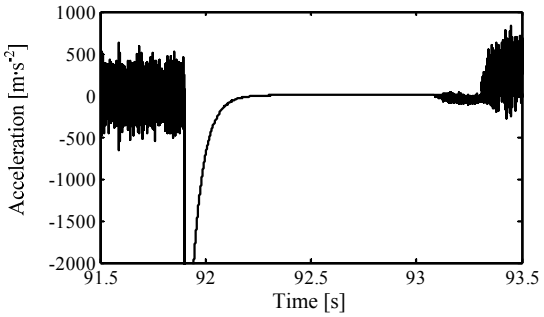

Fig.6. The vibration signal segment during which accelerometer failed.

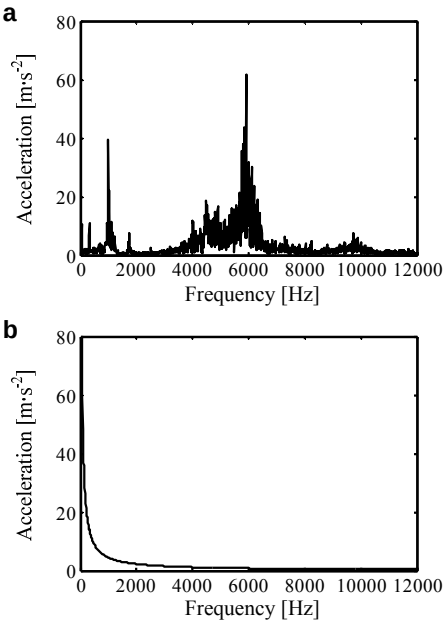

Fig.7. Amplitude spectrum: (a) before sensor malfunction and (b) after sensor malfunction.

two spectra, the standard deviation of spectrum sequence in this frequency band is used as the first feature for identifying sensor malfunction. Fig. 8 shows the standard deviation of the spectrum (between 3 000 Hz and 7 000 Hz) of the tangential vibration of test T618. It can be seen that the values for sensor malfunction reduce from about 16 to nearly 0, showing that the standard deviation can be an effective feature.

Although three vibration signals are at three different directions, axial direction, radial direction and tangential direction, as these signals are sampled synchronously, they should be synchronous correlative to same degree no matter whether the turbopump is normal or not. If one of these sensors failed, the synchronous correlation between the signal sampled with this fault sensor and the other signals would decrease significantly. Thus the synchronous correlation can be selected as a feature to recognize sensor malfunction. For two synchronous signals s_i and s_j, their absolute correlation coefficient $C_{i,j}$ can be calculated by

$$C_{i,j} = \frac{\left|Cov(s_i, s_j)\right|}{\sigma(s_i)\sigma(s_j)} \tag{13}$$

where $Cov(s_i, s_j)$ is the covariance of s_i and s_j, $\sigma(s_i)$ and $\sigma(s_j)$ are the standard deviations of s_i and s_j. Signals s_i and s_j are correlative if $C_{i,j} > 0$. And signals s_i and s_j are not correlative if $C_{i,j} = 0$. Fig. 9 shows the synchronous correlation coefficients of vibration signals during test T618. It can be seen that the vibration signals are correlative when the sensors are normal. On the contrary, when one of the sensors fails, the absolute correlation coefficient drops to 0 and the vibration signals are not correlative any more.

3.2 Support vector data description

Support vector machine (SVM) has been widely applied to machine health monitoring and fault diagnosis due to its global solution and excellent generalization [20]. OCSVM is the extension of SVM and it is used to resolve novelty detection problems. v-support vector classifier (v-SVC) and support vector data description (SVDD) are two equivalent OCSVMs. v-SVC is a model of hyper plane. The hyper plane is optimized to separate the data set from the origin with maximal margin. Test data lying on the side of the origin are labeled as novelties [21]. SVDD is a model of hyper sphere which is optimized to encompass almost all the normal data with the minimum radius. Test data outside the hyper sphere are labeled as novelties [22].

For the post analysis of turbopump test data, the hyper sphere of SVDD can be yielded by solving a quadratic optimization problem as

$$\underset{\alpha_i, \alpha_j}{\text{Minimize}}\ P(\alpha) = \sum_{i,j=1}^{l} \alpha_i \alpha_j K\left(\boldsymbol{x}_i, \boldsymbol{x}_j\right) \tag{14}$$

$$\text{Subject to } 0 \le \alpha_i, \alpha_j \le (vl)^{-1}, \sum_{i=1}^{l} \alpha_i = 1 \tag{15}$$

in which $\boldsymbol{x}_i$ and $\boldsymbol{x}_j$ are training vectors, α_i and α_j are the corresponding Lagrange multipliers, $v \in (0, 1)$ is the trade-off parameter. As v is the upper bound on the fraction of outliers over all training samples, it can be used to control the trade-off between the volume of the sphere and the number of outliers [23]. Solving such a quadratic problem means finding a set $\{\alpha_i\}$ that minimizes $P(\alpha)$ with subject to the constraints of Eq. (15). Training vectors with $\alpha = 0$, $0 < \alpha < (vl)^{-1}$, and $\alpha = (vl)^{-1}$ are respectively named as non-support vectors (NSV), boundary support vectors (BSV), and non-boundary support vectors (NBSV) and they are respectively located in the sphere, on the sphere and outside the sphere.

The decision function or test function of SVDD is

$$f(\boldsymbol{z}) = \sum\nolimits_k \alpha_k K\left(\boldsymbol{x}_k, \boldsymbol{z}\right) - b \tag{16}$$

where $\boldsymbol{z}$ is a test vector, $\boldsymbol{x}_k$ is one of BSVs or NBSVs, α_k is the corresponding Lagrange multiplier of $\boldsymbol{x}_k$, b is the threshold or offset. If $f(\boldsymbol{z}) \ge 0$, $\boldsymbol{z}$ will be accepted as a target sample, otherwise $\boldsymbol{z}$ will be excluded as a outlier. $f(\boldsymbol{z})$ is also considered as

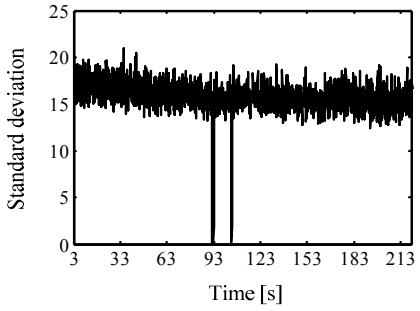

Fig.8. Standard deviation of the spectrum.

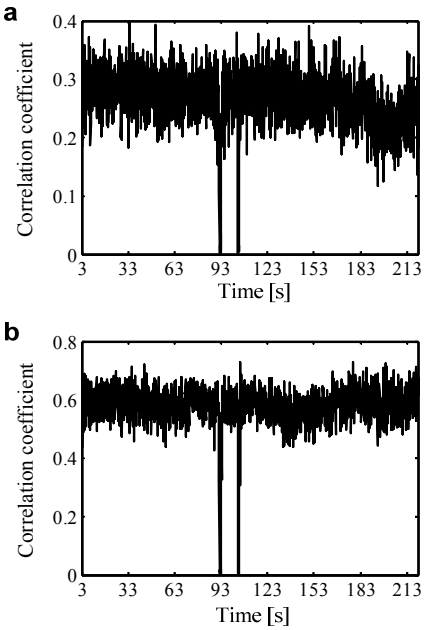

Fig.9. The synchronous correlation coefficients: (a) the correlation coefficient of the tangential vibration and the axial vibration; (b) the correlation coefficient of the tangential vibration and the radial vibration.

the novelty index of the sample **z**.

As BSVs lies on the sphere, the threshold can be yielded by inputting one of BSVs to the decision function:

$$b = \delta \cdot \sum_k \alpha_k K(\boldsymbol{x}_k, \boldsymbol{x}_{\mathrm{BSVs}}) \tag{17}$$

where δ is a scaling parameter used to decrease the threshold to reduce false alarms. δ can be set smaller than and close to 1.

SVDD mostly uses Gaussian kernel

$$K(\boldsymbol{x}_i, \boldsymbol{x}_j) = \exp\left(-\frac{\|\boldsymbol{x}_i - \boldsymbol{x}_j\|^2}{\sigma^2}\right) \tag{18}$$

where σ is the width parameter of the kernel. Methods used to optimize the parameters are studied extensively in Ref. [13] and have not been addressed in this study.

3.3 Post analysis results

The accelerometer at axial direction failed many times during test T626. The vibration signal from it, shown in Fig. 10, has many segments similar to the signal segment in Fig. 6. Target data used for training samples extraction are obtained by intercepting these signal segments from the original signal and appending them after each other. Signals on other directions are operated in the same way. Then features are calculated from the training data. The stars in Fig. 11 illustrate the extracted feature samples. The coordinate x_1 is the standard deviation of the spectrum and coordinates x_2 and x_3 are respectively the synchronous correlation coefficients of the target vibration signal and its synchronous vibration signals.

According to results of cross validation, parameters of the SVDD are set as $\nu = 0.01$, $\sigma = 2$ and $\delta = 0.98$. Training SVDD with these samples yields the description model as shown by the grid in Fig. 11. Supposing $f(\mathbf{z})$ is the decision function of the model, which is also the sensor malfunction index, sensor malfunction can be detected if $f(\mathbf{z}) > 0$.

The validity of this description model should be examined in two respects. First of all, sensor fault should be discriminated from faults of the turbopump. Fig. 12 shows the detection results of the tangential vibration in test T618 with the description model. Feature samples used for detection are shown in Fig. 8 and Fig. 9. It can be seen from Fig. 12 that the sensor fault indexes turn to be positive at 91.9 seconds and 104.1 seconds. This means that the novel events detected (as shown in Fig. 4d) are identified as sensor fault.

Secondly, the turbopump faults should not be labeled as sensor fault. Fig. 13 shows the sensor fault features of the axial vibration in test T627 and their fault indexes. The sensor fault indexes in Fig. 13d show negative values in the whole time range. This means that the novel events detected are not sensor fault but fault of the turbopump.

3.4 Discussion

As shown in online monitoring results in section 2.3, sensor malfunctions can be detected as novelties with the adaptive Gaussian threshold model, but the adaptive Gaussian threshold model cannot separate sensor malfunctions from faults of the turbopumps. Thus sensor malfunctions cause false alarms during online health monitoring of the turbopumps. Sensor malfunctions should be separated from turbopump faults not only during post analysis but also during online health monitoring. At present, the field engineer does not shut the engine as long as the online monitoring system alarms. The field engineer has to make an aggregate decision according to not only the online monitoring results of vibration, but also other factors such as the rotational speed of the turbopump and the hydraulic parameters of the fuel/oxygen fill-in systems. Future research involves recognition of sensor malfunctions during online health monitoring.

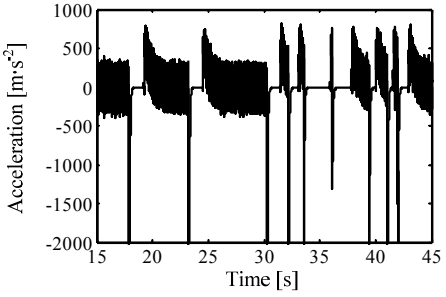

Fig.10. The axial vibration signal of the test T626 during which the accelerometer failed many times.

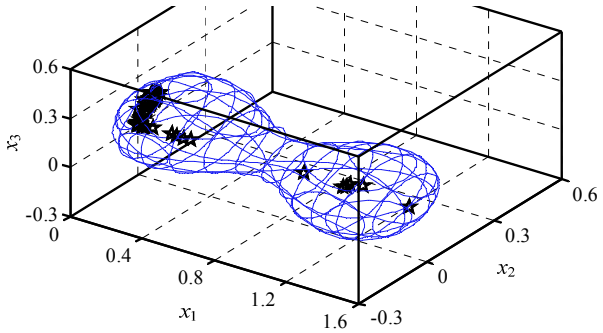

Fig.11. The description of the sensor malfunction. Reticular grid is the decision boundary, stars in reticular grid the are extracted feature vectors, x_1 is the standard deviation of vibration spectrum, x_2 and x_3 are respectively the synchronous correlation coefficients of the target vibration signal and its synchronous vibration signals.

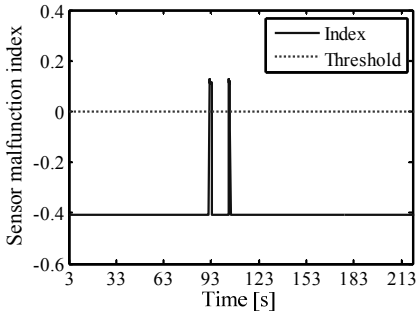

Fig.12. The sensor fault index of the tangential vibration in test T618.

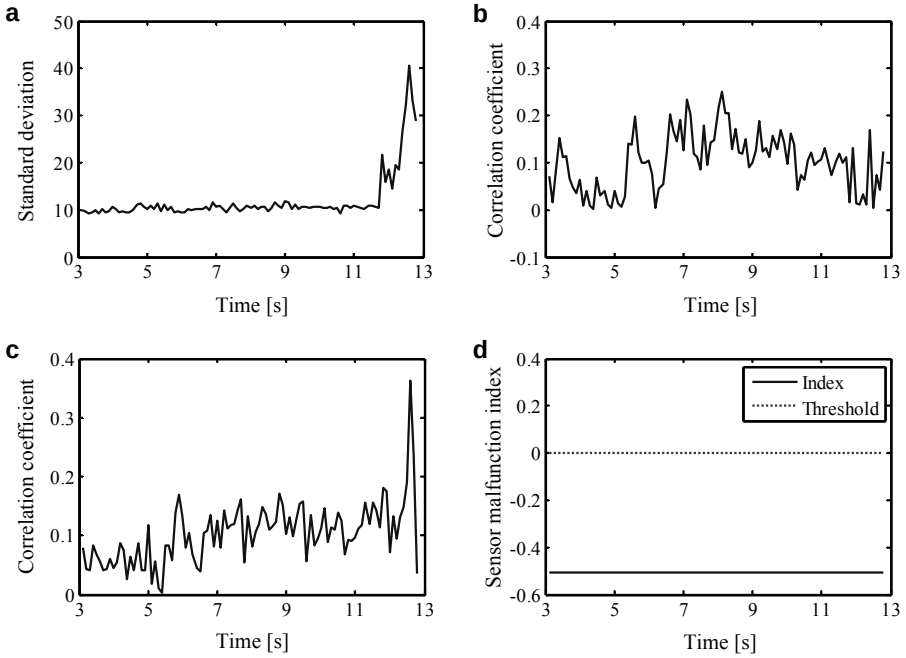

Fig.13. The sensor fault features and their fault index of the axial vibration in test T627

4. Conclusions

In this paper, two novelty detection methods are presented for both online health monitoring and post analysis of vibration signals for turbopump health monitoring. The first method is the adaptive Gaussian threshold model used for online health monitoring. This method is designed to learn online the characteristics of statistical features including RMS, kurtosis factor and crest factor and subsequently implement health monitoring. Health monitoring results showed that this method is able to recognize novel events in vibration signals, including rub-impact fault and sensor malfunction. Compared with the incremental adaptive threshold model the proposed method is more sensitive and is of less computational complexity.

The second method is OCSVM based offline diagnosis. This method is used for post analysis of the vibration signals to differentiate sensor faults from faults of the turbopump. The standard deviation of spectrum and the correlative coefficients of the target signal and its synchronous signals are extracted as features for sensor fault identification. A description model is obtained by training OCSVM with these features. By applying this model to full historical datasets, the results show that all of turbopump faults that have happened for the data sets that were investigated can be discriminated from sensor fault.

Acknowledgment

This work was supported by the National Natural Science Foundation of China [grant numbers 51105366] and the Research Project of National University of Defense Technology [grant number JC12-03-02]. The authors appreciate sincerely the reviewers' comments that helped us improve the paper.

References

[1] M. Markou and S. Singh, Novelty detection: a review, Part 1: statistical approaches, *Signal Processing* 83 (2003) 2481-2497.

[2] K. Worden, G. Manson, and D. Allman, Experimental validation of a structural health monitoring methodology, Part I: Novelty detection on a laboratory structure, *Journal of Sound and Vibration* 259 (2003) 323-343.

[3] L. Tarassenko, A. Nairac, N. Townsend, and P. Cowley, Novelty detection in jet engines, *IEE Colloquium on Condition Monitoring, Imagery, External Structures and Health* 1999 41-45.

[4] A. Srivastava, Discovering system health anomalies using data mining techniques, *Proceedings of the Joint Army Navy NASA Air Force Conference on Propulsion*, Charleston, SC, June 2005.

[5] D. Clifton, P. Bannister, and L. Tarassenko, Novelty detection in large-vehicle turbocharger operation, *IEA/AIE* 2007 591- 600.

[6] C. Surace and K. Worden, Novelty detection in a changing environment: a negative selection approach, *Mechanical Systems and Signal Processing* 24 (2010) 1114–1128.

[7] S. J. Hickinbotham and J. Austin, Neural networks for novelty detection in airframe strain data, *Proceeding of IEEE IJCNN*, 2000.

[8] M. Wong, L. B. Jack, and A. K. Nandi, Modified self-

organising map for automated novelty detection applied to vibration signal monitoring, *Mechanical Systems and Signal Processing* 20 (2006) 593-610.

[9] P. Hayton, B. Schölkopf, L. Tarassenko, and et al., Support vector novelty detection applied to jet engine vibration spectra, *Advances in Neural Information Processing Systems* 13, 2001.

[10] P. Hayton, S. Utete, D. King, and et al., Static and dynamic novelty detection methods for jet engine health monitoring, *Philosophical transactions of the royal society, a-mathematical physical and engineering sciences* 365 (2007) 493-514.

[11] M. Markou, S. Singh, Novelty detection: a review, Part 2: neural network based approaches, *Signal Processing*, 83 (2003) 2499-2521.

[12] Hu Lei, Hu Niaoqing, Qin Guojun, and Gu Fengshou, Turbopump condition monitoring using incremental clustering and one-class support vector machine, *Chinese Journal of Mechanical Engineering* 24 (3) (2011) 169-173.

[13] D. Tax, One-class classification, Ph.D. Dissertation, Delft University of Technology 2001.

[14] A. Muszynska, Rotor-to-stationary elment rub-related vibration phenomena in rotating machinery - literature survey, *The Shock and Vibration Digest* 21 (1989) 3-11.

[15] N. Q. Hu, Research on identification of nonlinear behavior and fault of rub-impact in rotors, Ph.D. Dissertation, National University of Defense Technology of China, 2001. (in Chinese)

[16] P. D. Samuel and D. J. Pines, A review of vibration-based techniques for helicopter transmission diagnostics, *Journal of Sound and Vibration* 282 (2005) 475-508.

[17] Davy M, Desobry F, Gretton A, et al. An online support vector machine for abnormal events detection [J]. *Signal Processing*, 86(2006) 2009-2025.

[18] G. J. Xie, Research on real-time fault detection technology and system for liquid rocket engine turbopump, Ph.D. Dissertation, National University of Defense Technology of China, 2006. (in Chinese)

[19] J. Kullaa, Sensor validation using minimum mean square error estimation, *Mechanical Systems and Signal Processing* 24 (2010) 1444-1457.

[20] A. Widodo and B. S. Yang, Support vector machine in machine condition monitoring and fault diagnosis, *Mechanical System and Signal Processing* 21 (2007) 2560-2574.

[21] B. Schölkopf, R. Williamson, A. Smola, and et al., Support vector method for novelty detection, *Advances in neural information processing systems 12: proceedings of the 1999 conference*, MIT Press, 2000 582-588.

[22] D. Tax and R. Duin, Support vector data description, *Machine Learning* 54 (2004) 45-66.

[23] S. K. Chu, Scaling up support vector data description by using Core-sets, Ph.D. Dissertation, Hong Kong University of Science and Technology, 2004.

Hu Lei, born in 1981, is currently a lecturer in National University of Defense Technology, China. He received his PhD degree from National University of Defense Technology in 2010. His research interests focus on mechanical signal processing, health monitoring, fault diagnostics and prognostics.